2. RECIPROCAL SPACE IN CRYSTAL-STRUCTURE DETERMINATION
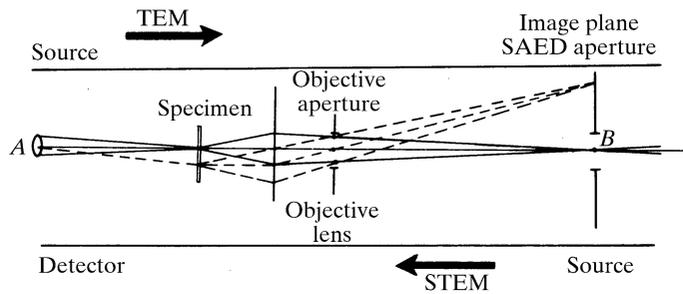

Fig. 2.5.2.2. Diagram representing the critical components of a conventional transmission electron microscope (TEM) and a scanning transmission electron microscope (STEM). For the TEM, electrons from a source A illuminate the specimen and the objective lens forms an image of the transmitted electrons on the image plane, B. For the STEM, a source at B is imaged by the objective lens to form a small probe on the specimen and some part of the transmitted beam is collected by a detector at A.

$$\Psi_0(u, v) \cdot T(u, v), \qquad (2.5.2.31)$$

where $\Psi_0(u, v)$ is the Fourier transform of $\psi_0(x, y)$ and $T(u, v)$ is the transfer function of the lens, consisting of an aperture function

$$A(u, v) = \begin{cases} 1 & \text{for } (u^2 + v^2)^{1/2} \leq A \\ 0 & \text{elsewhere} \end{cases} \qquad (2.5.2.32)$$

and a phase function $\exp\{i\chi(u, v)\}$ where the phase perturbation $\chi(uv)$ due to lens defocus Δf and aberrations is usually approximated as

$$\chi(uv) = \pi \cdot \Delta f \cdot \lambda(u^2 + v^2) + \frac{\pi}{2} C_s \lambda^3 (u^2 + v^2)^2, \qquad (2.5.2.33)$$

and u, v are the reciprocal-space variables related to the scattering angles φ_x, φ_y by

$$u = (\sin \varphi_x)/\lambda,$$
$$v = (\sin \varphi_y)/\lambda.$$

The image amplitude distribution, referred to the object coordinates, is given by Fourier transform of (2.5.2.31) as

$$\psi(xy) = \psi_0(xy) * t(xy), \qquad (2.5.2.34)$$

where $t(xy)$, given by Fourier transform of $T(u, v)$, is the spread function. The image intensity is then

$$I(xy) = |\psi(xy)|^2 = |\psi_0(xy) * t(xy)|^2. \qquad (2.5.2.35)$$

In practice the coherent imaging theory provides a good approximation but limitations of the coherence of the illumination have appreciable effects under high-resolution imaging conditions.

The variation of focal lengths according to (2.5.2.30) is described by a function $G(\Delta f)$. Illumination from a finite incoherent source gives a distribution of incident-beam angles $H(u_1, v_1)$. Then the image intensity is found by integrating incoherently over Δf and u_1, v_1:

$$I(xy) = \int \int G(\Delta f) \cdot H(u_1 v_1)$$
$$\times |\mathscr{F}\{\Psi_0(u - u_1, v - v_1) \cdot T_{\Delta f}(u, v)\}|^2 \, d(\Delta f) \cdot du_1 \, dv_1, \qquad (2.5.2.36)$$

where $\mathscr{F}$ denotes the Fourier-transform operation.

In the scanning transmission electron microscope (STEM), the objective lens focuses a small bright source of electrons on the object and directly transmitted or scattered electrons are detected to form an image as the incident beam is scanned over the object (see Fig. 2.5.2.2). Ideally the image amplitude can be related to that of the conventional transmission electron microscope by use of the 'reciprocity relationship' which refers to point sources and detectors for scalar radiation in scalar fields with elastic scattering processes only. It may be stated: 'The amplitude at a point B due to a point source at A is identical to that which would be produced at A for the identical source placed at B'.

For an axial point source, the amplitude distribution produced by the objective lens on the specimen is

$$\mathscr{F}[T(u, v)] = t(xy). \qquad (2.5.2.37)$$

If this is translated by the scan to X, Y, the transmitted wave is

$$\psi_0(xy) = q(xy) \cdot t(x - X, y - Y). \qquad (2.5.2.38)$$

The amplitude on the plane of observation following the specimen is then

$$\Psi(uv) = Q(u, v) * \{T(uv) \exp[2\pi i(uX + vY)]\}, \qquad (2.5.2.39)$$

and the image signal produced by a detector having a sensitivity function $H(u, v)$ is

$$I(X, Y) = \int H(u, v)|Q(u, v) * T(u, v)$$
$$\times \exp\{2\pi i(uX + vY)\}|^2 \, du \, dv. \qquad (2.5.2.40)$$

If $H(u, v)$ represents a small detector, approximated by a delta function, this becomes

$$I(x, y) = |q(xy) * t(xy)|^2, \qquad (2.5.2.41)$$

which is identical to the result (2.5.2.35) for a plane incident wave in the conventional transmission electron microscope.

2.5.2.7. Imaging of very thin and weakly scattering objects

(*a*) *The weak-phase-object approximation.* For sufficiently thin objects, the effect of the object on the incident-beam amplitude may be represented by the transmission function (2.5.2.16) given by the phase-object approximation. If the fluctuations, $\varphi(xy) - \bar{\varphi}$, about the mean value of the projected potential are sufficiently small so that $\sigma[\varphi(xy) - \bar{\varphi}] \ll 1$, it is possible to use the *weak-phase-object approximation* (WPOA)

$$q(xy) = \exp\{-i\sigma\varphi(xy)\} = 1 - i\sigma\varphi(xy), \qquad (2.5.2.42)$$

where $\varphi(xy)$ is referred to the average value, $\bar{\varphi}$. The assumption that only first-order terms in $\sigma\varphi(xy)$ need be considered is the equivalent of a single-scattering, or kinematical, approximation applied to the two-dimensional function, the projected potential
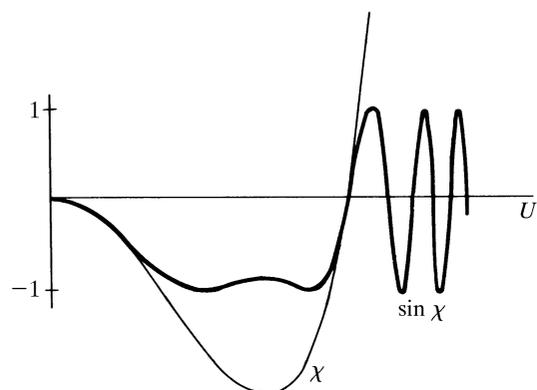
Fig. 2.5.2.3. The functions $\chi(U)$, the phase factor for the transfer function of a lens given by equation (2.5.2.33), and $\sin \chi(U)$ for the Scherzer optimum defocus condition, relevant for weak phase objects, for which the minimum value of $\chi(U)$ is $-2\pi/3$.

of (2.5.2.16). From (2.5.2.42), the image intensity (2.5.2.35) becomes

$$I(xy) = 1 + 2\sigma\varphi(xy) * s(xy), \qquad (2.5.2.43)$$

where the spread function $s(xy)$ is the Fourier transform of the imaginary part of $T(uv)$, namely $A(uv)\sin \chi(uv)$.

The optimum imaging condition is then found, following Scherzer (1949), by specifying that the defocus should be such that $|\sin \chi|$ is close to unity for as large a range of $U = (u^2 + v^2)^{1/2}$ as possible. This is so for a negative defocus such that $\chi(uv)$ decreases to a minimum of about $-2\pi/3$ before increasing to zero and higher as a result of the fourth-order term of (2.5.2.33) (see Fig. 2.5.2.3). This optimum, 'Scherzer defocus' value is given by

$$\frac{d\chi}{du} = 0 \quad \text{for} \quad \chi = -2\pi/3$$

or

$$\Delta f = -\left(\tfrac{4}{3}C_s\lambda\right)^{1/2}. \qquad (2.5.2.44)$$

The resolution limit is then taken as corresponding to the value of $U = 1.51 C_s^{-1/4}\lambda^{-3/4}$ when $\sin \chi$ becomes zero, before it begins to oscillate rapidly with U. The resolution limit is then

$$\Delta x = 0.66 C_s^{1/4}\lambda^{3/4}. \qquad (2.5.2.45)$$

For example, for $C_s = 1$ mm and $\lambda = 2.51 \times 10^{-2}$ Å (200 keV), $\Delta x = 2.34$ Å.

Within the limits of the WPOA, the image intensity can be written simply for a number of other imaging modes in terms of the Fourier transforms $c(\mathbf{r})$ and $s(\mathbf{r})$ of the real and imaginary parts of the objective-lens transfer function $T(\mathbf{u}) = A(\mathbf{u})\exp\{i\chi(\mathbf{u})\}$, where $\mathbf{r}$ and $\mathbf{u}$ are two-dimensional vectors in real and reciprocal space, respectively.

For dark-field TEM images, obtained by introducing a central stop to block out the central beam in the diffraction pattern in the back-focal plane of the objective lens,

$$I(\mathbf{r}) = [\sigma\varphi(\mathbf{r}) * c(\mathbf{r})]^2 + [\sigma\varphi(\mathbf{r}) * s(\mathbf{r})]^2. \qquad (2.5.2.46)$$

Here, as in (2.5.2.42), $\varphi(\mathbf{r})$ should be taken to imply the difference from the mean potential value, $\varphi(\mathbf{r}) - \bar{\varphi}$.

For bright-field STEM imaging with a very small detector placed axially in the central beam of the diffraction pattern (2.5.2.39) on the detector plane, the intensity, from (2.5.2.41), is given by (2.5.2.43).

For a finite axially symmetric detector, described by $D(\mathbf{u})$, the image intensity is

$$I(\mathbf{r}) = 1 + 2\sigma\varphi(\mathbf{r}) * \{s(\mathbf{r})[d(\mathbf{r}) * c(\mathbf{r})] - c(\mathbf{r})[d(\mathbf{r}) * s(\mathbf{r})]\}, \qquad (2.5.2.47)$$

where $d(\mathbf{r})$ is the Fourier transform of $D(\mathbf{u})$ (Cowley & Au, 1978).

For STEM with an annular dark-field detector which collects all electrons scattered outside the central spot of the diffraction pattern in the detector plane, it can be shown that, to a good approximation (valid except near the resolution limit)

$$I(\mathbf{r}) = \sigma^2\varphi^2(\mathbf{r}) * [c^2(\mathbf{r}) + s^2(\mathbf{r})]. \qquad (2.5.2.48)$$

Since $c^2(\mathbf{r}) + s^2(\mathbf{r}) = |t(\mathbf{r})|^2$ is the intensity distribution of the electron probe incident on the specimen, (2.5.2.48) is equivalent to the incoherent imaging of the function $\sigma^2\varphi^2(\mathbf{r})$.

Within the range of validity of the WPOA or, in general, whenever the zero beam of the diffraction pattern is very much stronger than any diffracted beam, the general expression (2.5.2.36) for the modifications of image intensities due to limited coherence may be conveniently approximated. The effect of integrating over the variables $\Delta f, u_1, v_1$, may be represented by multiplying the transfer function $T(u, v)$ by so-called 'envelope functions' which involve the Fourier transforms of the functions $G(\Delta f)$ and $H(u_1, v_1)$.

For example, if $G(\Delta f)$ is approximated by a Gaussian of width ε (at e^{-1} of the maximum) centred at Δf_0 and $H(u_1v_1)$ is a circular aperture function

$$H(u_1v_1) = \begin{cases} 1 & \text{if } u_1, v_1 < b \\ 0 & \text{otherwise}, \end{cases}$$

the transfer function $T_0(uv)$ for coherent radiation is multiplied by

$$\exp\{-\pi^2\lambda^2\varepsilon^2(u^2 + v^2)^2/4\} \cdot J_1(\pi B\eta)/(\pi B\eta)$$

where

$$\eta = f_0\lambda(u + v) + C_s\lambda^3(u^3 + v^3)$$
$$+ \pi i\varepsilon^2\lambda^2(u^3 + u^2v + uv^2 + v^3)/2. \qquad (2.5.2.49)$$

(b) *The projected charge-density approximation.* For very thin specimens composed of moderately heavy atoms, the WPOA is inadequate. Within the region of validity of the phase-object approximation (POA), more complicated relations analogous to (2.5.2.43) to (2.5.2.47) may be written. A simpler expression may be obtained by use of the two-dimensional form of Poisson's equation, relating the projected potential distribution $\varphi(xy)$ to the projected charge-density distribution $\rho(xy)$. This is the PCDA (projected charge-density approximation) (Cowley & Moodie, 1960),

$$I(xy) = 1 + 2\Delta f \cdot \lambda\sigma\rho(xy). \qquad (2.5.2.50)$$

This is valid for sufficiently small values of the defocus Δf, provided that the effects of the spherical aberration may be neglected, *i.e.* for image resolutions not too close to the Scherzer

resolution limit (Lynch *et al.*, 1975). The function $\rho(xy)$ includes contributions from both the positive atomic nuclei and the negative electron clouds. For underfocus (Δf negative), single atoms give dark spots in the image. The contrast reverses with defocus.

2.5.2.8. Crystal structure imaging

(*a*) *Introduction*. It follows from (2.5.2.43) and (2.5.2.42) that, within the severe limitations of validity of the WPOA or the PCDA, images of very thin crystals, viewed with the incident beam parallel to a principal axis, will show dark spots at the positions of rows of atoms parallel to the incident beam. Provided that the resolution limit is less than the projected distances between atom rows (1–3 Å), the projection of the crystal structure may be seen directly.

In practice, theoretical and experimental results suggest that images may give a direct, although nonlinear, representation of the projected potential or charge-density distribution for thicknesses much greater than the thicknesses for validity of these approximations, *e.g.* for thicknesses which may be 50 to 100 Å for 100 keV electrons for 3 Å resolutions and which increase for comparable resolutions at higher voltage but decrease with improved resolutions.

The use of high-resolution imaging as a means for determining the structures of crystals and for investigating the form of the defects in crystals in terms of the arrangement of the atoms has become a widely used and important branch of crystallography with applications in many areas of solid-state science. It must be emphasized, however, that image intensities are strongly dependent on the crystal thickness and orientation and also on the instrumental parameters (defocus, aberrations, alignment *etc.*). It is only when all of these parameters are correctly adjusted to lie within strictly defined limits that interpretation of images in terms of atom positions can be attempted [see *IT* C (2004, Section 4.3.8)].

Reliable interpretations of high-resolution images of crystals ('crystal structure images') may be made, under even the most favourable circumstances, only by the comparison of observed image intensities with intensities calculated by use of an adequate approximation to many-beam dynamical diffraction theory [see *IT* C (2004, Section 4.3.6)]. Most calculations for moderate or large unit cells are currently made by the multislice method based on formulation of the dynamical diffraction theory due to Cowley & Moodie (1957). For smaller unit cells, the matrix method based on the Bethe (1928) formulation is also frequently used (Hirsch *et al.*, 1965).

(*b*) *Fourier images*. For periodic objects in general, and crystals in particular, the amplitudes of the diffracted waves in the back focal plane are given from (2.5.2.31) by

$$\Psi_0(\mathbf{h}) \cdot T(\mathbf{h}). \qquad (2.5.2.51)$$

For rectangular unit cells of the projected unit cell, the vector $\mathbf{h}$ has components h/a and k/b. Then the set of amplitudes (2.5.2.34), and hence the image intensities, will be identical for two different sets of defocus and spherical aberration values Δf_1, C_{s1} and Δf_2, C_{s2} if, for an integer N,

$$\chi_1(h) = \chi_2(h) = 2N\pi;$$

i.e.

$$\pi\lambda\left(\frac{h^2}{a^2} + \frac{k^2}{b^2}\right)(\Delta f_1 - \Delta f_2) + \frac{1}{2}\pi\lambda^3\left(\frac{h^2}{a^2} + \frac{k^2}{b^2}\right)^2(C_{s1} - C_{s2}) = 2\pi N.$$

This relationship is satisfied for all h, k if a^2/b^2 is an integer and

$$\Delta f_1 - \Delta f_2 = 2na^2/\lambda$$

and

$$C_{s1} - C_{s2} = 4ma^4/\lambda^3, \qquad (2.5.2.52)$$

where m, n are integers (Kuwabara, 1978). The relationship for Δf is an expression of the Fourier image phenomenon, namely that for a plane-wave incidence, the intensity distribution for the image of a periodic object repeats periodically with defocus (Cowley & Moodie, 1960). Hence it is often necessary to define the defocus value by observation of a nonperiodic component of the specimen such as a crystal edge (Spence *et al.*, 1977).

For the special case $a^2 = b^2$, the image intensity is also reproduced exactly for

$$\Delta f_1 - \Delta f_2 = (2n + 1)a^2/\lambda, \qquad (2.5.2.53)$$

except that in this case the image is translated by a distance $a/2$ parallel to each of the axes.

2.5.2.9. Image resolution

(1) *Definition and measurement*. The 'resolution' of an electron microscope or, more correctly, the 'least resolvable distance', is usually defined by reference to the transfer function for the coherent imaging of a weak phase object under the Scherzer optimum defocus condition (2.5.2.44). The resolution figure is taken as the inverse of the U value for which $\sin\chi(U)$ first crosses the axis and is given, as in (2.5.2.45), by

$$\Delta x = 0.66 C_s^{1/4}\lambda^{3/4}. \qquad (2.5.2.45)$$

It is assumed that an objective aperture is used to eliminate the contribution to the image for U values greater than the first zero crossing, since for these contributions the relative phases are distorted by the rapid oscillations of $\sin\chi(U)$ and the corresponding detail of the image is not directly interpretable in terms of the projection of the potential distribution of the object.

The resolution of the microscope in practice may be limited by the incoherent factors which have the effect of multiplying the WPOA transfer function by envelope functions as in (2.5.2.49).

The resolution, as defined above, and the effects of the envelope functions may be determined by Fourier transform of the image of a suitable thin, weakly scattering amorphous specimen. The Fourier-transform operation may be carried out by use of an optical diffractometer. A more satisfactory practice is to digitize the image directly by use of a two-dimensional detector system in the microscope or from a photographic recording, and perform the Fourier transform numerically.

For the optical diffractometer method, the intensity distribution obtained is given from (2.5.2.43) as a radially symmetric function of U,

$$I(U) = |\mathscr{F}I(xy)|^2$$
$$= \delta(U) + 4\sigma^2|\Phi(u)|^2 \cdot \sin^2\chi(U) \cdot E^2(U), \qquad (2.5.2.54)$$

where $E(U)$ is the product of the envelope functions.

In deriving (2.5.2.54) it has been assumed that:
(*a*) the WPOA applies;
(*b*) the optical transmission function of the photographic record is linearly related to the image intensity, $I(xy)$;